A New Inverse Method for Determining Uniaxial Flow Properties by Spherical Indentation Test

Guoyao Chen
East China University of Science and Technology
Xiaocheng Zhang
East China University of Science and Technology
Jiru Zhong
East China University of Science and Technology
Kaishu Guan (guankaishu@ecust.edu.cn)
East China University of Science and Technology

Original Article

Keywords: Spherical indentation test, Database method, Uniaxial stress-strain relationship

Posted Date: January 9th, 2021

DOI: https://doi.org/10.21203/rs.3.rs-141379/v1

A new inverse method for determining uniaxial flow properties by spherical indentation test

Guoyao Chen[a], Xiaochen Zhang[a], Jiru Zhong[a*], Kaishu Guan [a*1]

a. School of Mechanical and Power Engineering, East China University of Science and Technology, Shanghai, 200237, China

ABSTRACT

This study presents a new inverse method to determine tensile flow properties from a single indentation force-depth curves. A database is established to replace the iterative FE calculations in conventional inverse methods and therefore can process the indentation data more quickly and easily. An axisymmetric FE model is constructed to simulate the elastic-plastic response of indention. Assuming the materials follow Ludwic constitutive model, by systematically changing the material parameters, numerous indentation force-depth curves are extracted from simulation results to establish the database. For a given experimental indentation curves, a mean square error (MSE) is designated to evaluate the deviations between the experimental curve and each curve in the database. Then, the relation of deviations versus stresses are investigated to acquire the true stresses at a series of plastic strain. To validate the new method, three different steels, i.e. A508, 316L and 2.25Cr1Mo are selected. Both simulated indentation curves and experimental indentation curves are used as inputs of the database to inversely acquire the flow properties. The result indicates that the proposed approach provides impressive accuracy when simulated indentation curves is used, but is less accurate when an experimental curve is used. This new method can quickly derive tensile properties without iterative calculations that yield a considerable computational costs and are therefore adaptive to engineering application.

Keywords: Spherical indentation test; Database method; Uniaxial stress-strain relationship.

* Corresponding author

E-mail address: zhongjiru@outlook.com (Jiru Zhong); guankaishu@ecust.edu.cn (Kaishu Guan)

1. Introduction

Indentation technique is generally take as a non-destructive method with the advantage of local characterization. It provides a feasible approach to determine the mechanical properties for in-service equipment [1-3], welded joints [4, 5], thin film materials [6-8], etc. The flow properties that describe the plastic hardening behaviors of materials have a widespread application in many cases such as structural design, numerical simulation and thus has been extensively investigated by indentation technique. Traditionally, the flow properties are obtained by establishing a conversion relationship between the indentation response and the elastic-plastic parameters of materials with empirical [1, 9-11] or analytical approaches [12-15]. However, such procedures are usually complicated due to the geometric and material nonlinearity and a significant contact problem (e.g. the effect of 'pile-up' and 'sink-in'). Moreover, the stress state under the indenter is definitely different from that from uniaxial tensile test, which increases the difficulties for evaluation of the flow curves from the indentation tests.

Recently, with the development of computational algorithms, several reverse strategies incorporating finite element simulations with optimum theory have been proposed. Based on the inverse tools, the material parameters can be directly extracted from the indentation response of materials without determining any equation that corresponds indentation response to the elastic-plastic parameters of materials. A commonly used tool is optimum algorithms [4, 6, 16-20]. Generally, the deviation between experimental and predictive data is considered as the objective function. And then an intelligence algorithm is employed to improve the predictive data by minimizing the objective value using the iterative FE simulations. J. Luo et.al. [18, 19]

firstly proposed the use of an optimization approach to extract the elastic-plastic parameters using a single loading-unloading indentation curve. Sun et.al. [4] determined the mechanical parameters of the weld zone with the micro-indentation data where the genetic algorithm (GA) is used for solving the inverse problem. Huang et.al. [17] employed the least-square difference between the experimental and simulated force-depth curve as the objective and identified the materials parameters with a modified particle swarm algorithm (PSO) which increases the ability to obtain a global optimal solution. Note that although these approaches have been widely reported, there are still several limitations. Firstly, an initial guess of material parameters is necessary and usually determined empirically and these values show a highly influence on the convergence speed. The improper guess values may impair the accuracy and efficiency of the algorithm. Secondly, it's possible that the iteration end up in a local optimum owing to the drawbacks of algorithms. More significantly, extensive iterative simulations for each parameter identification are required and therefore yield a considerable time and computational cost.

Another efficient inverse tool that are widely used is artificial neural networks (ANN) [21-23]. By adjusting the weights of connections between the artificial neurons, the ANN is trained by the data from finite element analyses. Then, the trained ANN was used to determine the material properties when presented with the indentation force-depth curves. The advantage of an ANN is that the material parameters can be quickly acquired as the corresponding indentation data is inputted. The structure of the ANN (i.e. dimension of the model input, and sizes of the network layer and neurons) has a greatly influence on the predictive ability. However, there is no specific rule for improving the structure of ANNs. What's more, transforming the inverse problem which refers to determine the flow properties from

indentation results into a network problem is always difficult.

In this study, a new method is presented to predict the flow properties from a single indention *F*-*h* curve where a database is used for solving the inverse problem. The database can replace the iterative algorithms to minimize the objective function and thus iterative FE simulations are not required in the new method. Firstly, by numerous finite element simulations with constitutive parameters varied systematically in a large range, a database that contain indentation force-depth curves is established. Then, by placing the experimental indentation response into the prepared database, a series of true stress plastic strain points are extracted. The feasibility of this new method was verified through a comparison of predicted tensile properties with the experimental tensile results using three steels.

2. Materials and experiments

Three steels, A508, 2.25Cr1Mo, 316L, which are commonly used in chemical industry, are researched in this study. The optical microstructures are shown in Fig. 1, indicating that the microstructure of SA508 steel consists of tempered bainite and 2.25Cr1Mo is bainite with a small amount of ferrite. 316L stainless steel is austenite equiaxed grains with a small amount of delta ferrite distributed on the grain boundaries. These steels are manufactured by forging process and therefore regarded as homogeneous and isotropic materials, which is also validated by these microstructures.

The tensile tests were conducted on these steels according to Chinese standard GB/T 228.1-2010. Specimens are fabricated into round bar with gauge radius 8mm and length 40mm. The loading procedures are controlled by displacement with a rate of 0.015mm/min at room temperature, which can be regarded as quasi-static process and thus viscoplastic effect is

neglected.

The spherical indentation tests are conducted using self-developed machine with a force resolution of 0.5N and displacement resolution of 0.1 μm. 50×10×10 mm specimens with the measuring surface paralleled to the bottle surface and polished by a 2000 grit sandpapers was adopted. A tungsten carbide spherical indenter with the diameter of 0.79 mm is used. A vertical displacement rate of 0.03mm/min is imposed to the indenter until the indented depth reaches to 12% of the indenter diameter, namely 0.0948mm. The experiments are slow and therefore considered as quasi-static process.

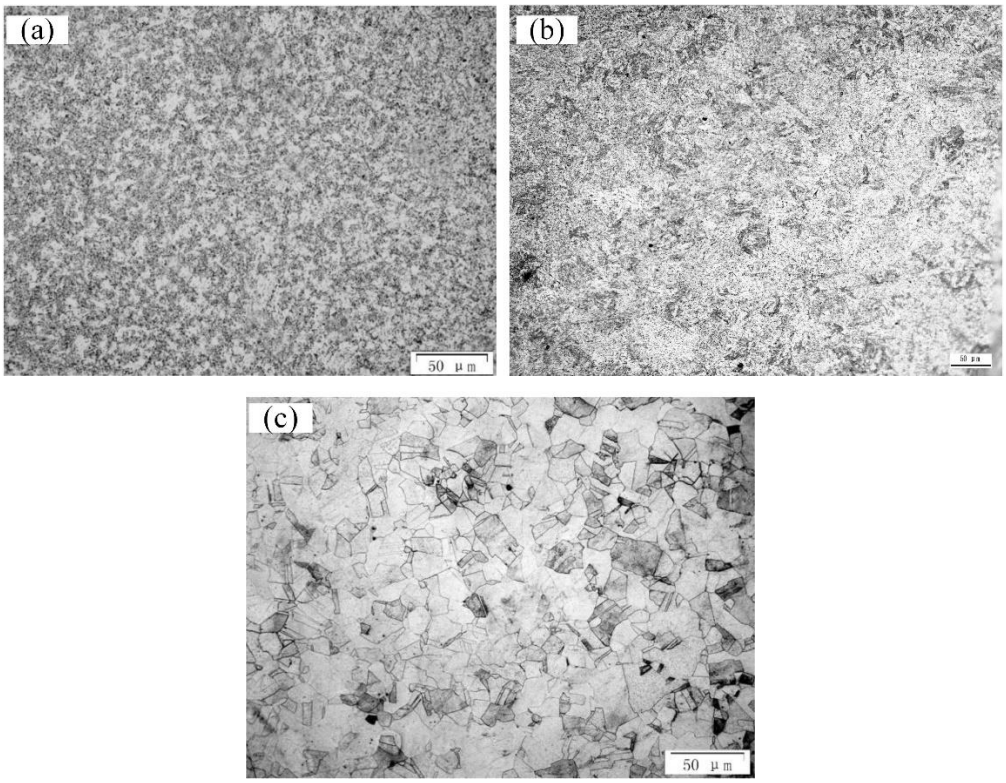

Fig. 1 The optical microstructures for (a) A508, (b) 316L and (c) 2.25Cr1Mo

3. Database approach modeling

3.1. Finite elements model

Taking the features of spherical indentation test into consideration, an axisymmetric model is adopted using ABAQUS/Standard 2018 to reduce the computational time (shown in Fig. 2).

The spherical indenter with a diameter of 0.79 mm is designated as an analytical rigid body since the deformation is generally ignored compared with the deformation of specimen. The specimen is modelled as a cylinder with the height of 3mm and the radius of 4 mm and meshed into over 7000 elements using CAX4R element type. To make a balance between the accuracy and computational cost of the model, the meshes are locally refined with 0.01 mm edge size element in the contact region and gradually coarse far away from the contact region. Constraint along the Y-axial is imposed to the bottom of the specimen. A vertical displacement was applied to the indenter until the indentation depth reaches to 0.0948mm (12% of the indenter diameter). The friction coefficient between the contact surfaces of specimen and indenter is fixed at 0.2 according to previous studies [16, 24].

In the elastic-plastic indentation simulations, material parameters including the Young's module *E*, Poisson's ratio ν, and the flow curve that describes the materials hardening behavior should be given. For most steels, the hardening behavior can be described by Ludwick hardening model:

$$\sigma = \sigma_0 + K\varepsilon_p^n \tag{1}$$

Here σ and ε_p are the true stress and true plastic strain, respectively. σ_0 is the initial yield strength, *K* is the strength coefficient and *n* denote the strain hardening exponent. Thus material constants in the FE model are characterized with a parameter vector $\boldsymbol{x} = [E, \nu, \sigma_0, K, n]^{\mathrm{T}}$. In fact, *E* and *v* have little influence on the FE results for commonly used steels. To reduce the computational cost, the Young's module *E* and Poisson's ratio ν are empirically fixed at 210000 MPa and 0.3 , respectively . The parameter vector is reduced to $\boldsymbol{x}=[\sigma_0, K, n]^{\mathrm{T}}$. To

establish a database that cover a wide range of materials, systemat0ically varied parameter vectors are used to create the Python script files with MATLAB code, and then the Python scripts are run by ABAQUS/Standard to acquire the force-depth curves. Over 20000 parameter vectors denoted by $\boldsymbol{x_j}$ $(1 \leq j \leq N)$ are used. N is the number of vectors in the database. Table 1 shows the range of varied parameters set.

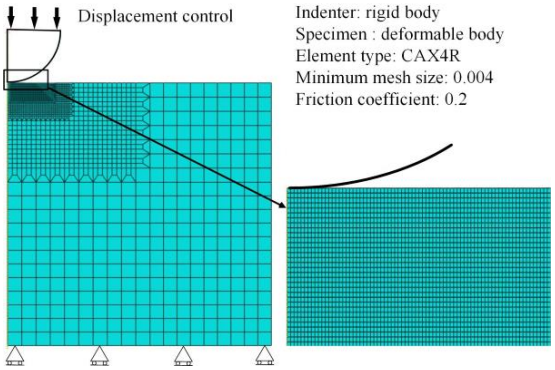

Fig. 2 Finite element model of Indentation tests

Table 1 Possible range of parameter vector $\boldsymbol{x_i}$ for the database

Constitutive model	Ludwik		
Parameters	σ_0 (MPa)	K (MPa)	n
Minimum value	100	100	0.06
Maximum value	880	1500	0.96
Interval	30	30	0.03

3.2. Procedures for uniaxial flow properties determination

Fig. 3 shows the schematic illustration for determining the flow properties of metal materials with a single *F-h* curve based on the application of the database. The FE model in the section 2.1 provides the indentation *F-h* curves of the database. When an experimental force-depth curve is prepared, a mean square error (MSE) is used to calculate the difference error between the force-depth curve in the database and that from experiments, which is defined as：

$$\begin{cases} f\left(\boldsymbol{x}_j\right)=\dfrac{1}{M}\displaystyle\sum_{i=1}^{M}\left(\dfrac{F_i^{\exp}-F_i^{\sin}\left(\boldsymbol{x}_j\right)}{F_i^{\exp}}\right)^2 \\ \boldsymbol{x}_j=[\sigma_0,K,n]^{\mathrm{T}} \text{ and } 1\le j\le N \end{cases} \tag{2}$$

Where $\boldsymbol{x}_j$ is the j_{th} vector, $\boldsymbol{x}_j=[\sigma_0,K,n]^{\mathrm{T}}$. $F_i^{\exp}$ and $F_i^{\sin}\left(\boldsymbol{x}_j\right)$ are the indentation forces at the depth of data point *i* for the experimental material and the j_{th} vector in the database. *M* is the total number of data points used in the indentation curve.

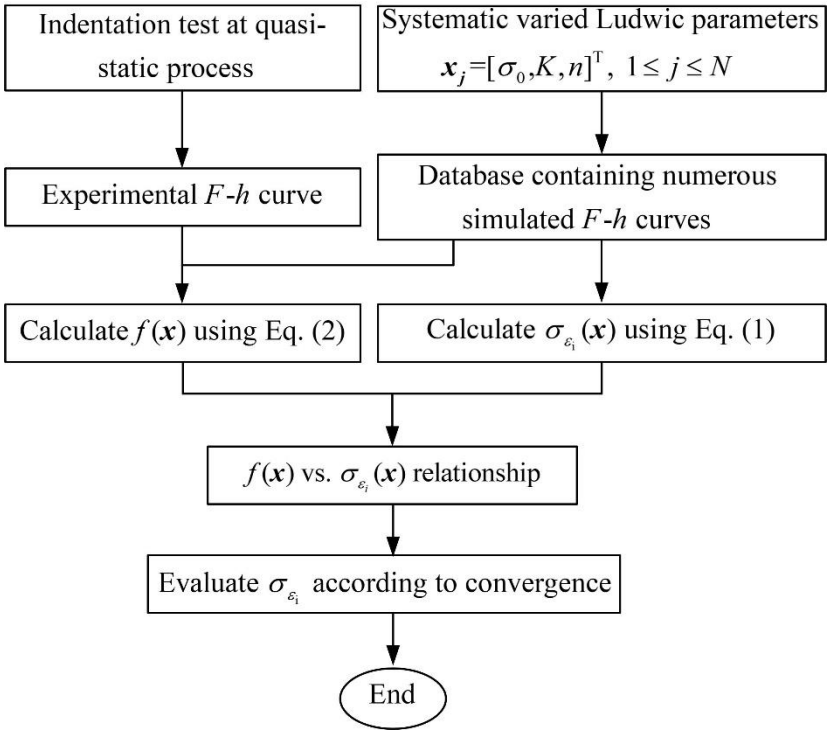

Fig. 3 flow chart for the new inverse method to determine the flow properties of metal materials

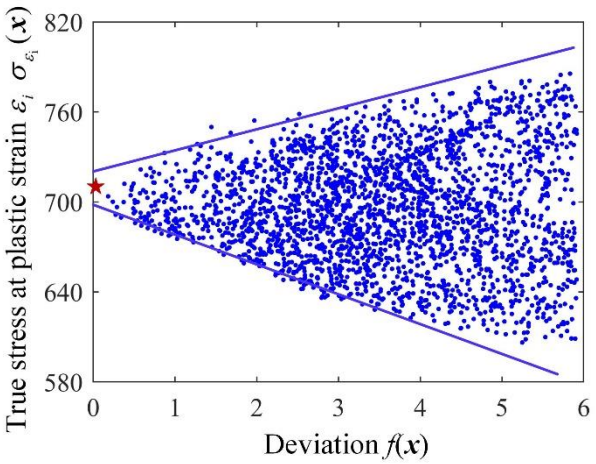

Fig. 4 Typical $f(\boldsymbol{x})$-$\sigma_{\varepsilon_i}(\boldsymbol{x})$ relationship indicating convergent $\sigma_{\varepsilon_i}(\boldsymbol{x})$ with decreasing $f(\boldsymbol{x})$

To describe the flow properties, a series of plastic strain values, namely ε_i =0.002,0.01,0.02,0.04,0.06,0.08,0.1,0.15,0.2,0.3,0.4,0.5 are selected and then the issues turns to the extraction of corresponding true stresses. The true stress correlated to ε_i for vector $\boldsymbol{x}$ in the database (denoted as $\sigma_{\varepsilon_i}(\boldsymbol{x})$) can be calculated with Eq. (1). To determine the true stress σ_{ε_i} of interesting material, the relation of $f(\boldsymbol{x})$ versus $\sigma_{\varepsilon_i}(\boldsymbol{x})$ are investigated in a two-dimensional coordinate system where the x and y-axis represent $f(\boldsymbol{x})$ and $\sigma_{\varepsilon_i}(\boldsymbol{x})$, respectively. Fig. 4 shows the typical $f(\boldsymbol{x})$-$\sigma_{\varepsilon_i}(\boldsymbol{x})$ relationship, which reveals that there exists an approximate linear lower and upper boundaries and the varied range of $\sigma_{\varepsilon_i}(\boldsymbol{x})$ is gradually narrow with decreasing $f(\boldsymbol{x})$. An appropriate explanation for this is that a smaller $f(\boldsymbol{x})$ means a better matched indentation curve with the experiment one and consequently results in a closer $\sigma_{\varepsilon_i}(\boldsymbol{x})$ to the experimental value. Ideally, when $f(\boldsymbol{x})$ is approximate to zero, $\sigma_{\varepsilon_i}(\boldsymbol{x})$ are tended to converge to an exact value, which can be regarded as the true stress correlated to ε_i for the experimental material. Notice that with the facts that the scale of the database is finite and the experimental curves are not definitely noise-free, $f(\boldsymbol{x})$ cannot be

zero. Here we specified a boundary line along the lower and upper boundary and employ the average value of the point of intersection of the boundary line and y-axis as the true stress the experimental material. According to a series of $f(\boldsymbol{x})$ vs. $\sigma_{\varepsilon_i}(\boldsymbol{x})$ relationships involving different plastic strain ε_i, the stresses at different plastic strains are extracted.

As can be seen from the procedures, the database replaced the costly iterative numerical inverse analysis, which therefore provides an easy, and quick route for measuring the flow properties compared with other inverse method. In addition, the prediction of local optimum is avoided since the new approach requires no initial guess of parameters and the parameter range in the database is enough wide.

4. Results and discussion

4.1 Uniaxial tensile and indentation results

According to the constant volume in plastic deformation, the true stress-strain curves are derived from the experimental engineering curves:

$$\begin{cases} \sigma = \sigma_{\mathrm{e}}(1+\varepsilon_{\mathrm{e}}) \\ \varepsilon = \ln(1+\varepsilon_{\mathrm{e}}) \end{cases} \tag{3}$$

Where σ and ε are true stress and strain，σ_{e} and ε_{e} are engineering stress and strain. Fig. 5 shows the true stress-strain curves for the three materials, which have definitely different plastic behaviors. It is noted that only the segment before necking are employed. A508 and 2.25Cr1Mo have relatively high yield strengths and low plastic deformation ability. On the contrast, S316L is good ductile material with a lower yield strength. In addition, A508 and 2.25Cr1Mo shows a good power law hardening behaviors, while linear hardening provides a

better description for 316L. Fig. 5 indicates that the fitting results of the three materials matched their true stress-strain well. The Ludwic fitting parameters are listed in Table 2.

The experimental *F-h* curves for the three materials are depicted in Fig. 6. It should be emphasized that the FE model used for construction of the database plays an important role in accurately predicting the tensile properties, since the database is employed to process the experimental indentation *F-h* curves. To validate the FE model, we employed the Ludwic parameters listed in Table 2 as inputs of FE model and extracted the simulated *F-h* curves. Fig. 6 shows that the simulated *F-h* curves, in general, agreed well with the corresponding experimental curves, indicating the accuracy of the FE model. For 316L, the simulated indentation data is a little higher than experimental one. This may result from the fitting error of tensile curves.

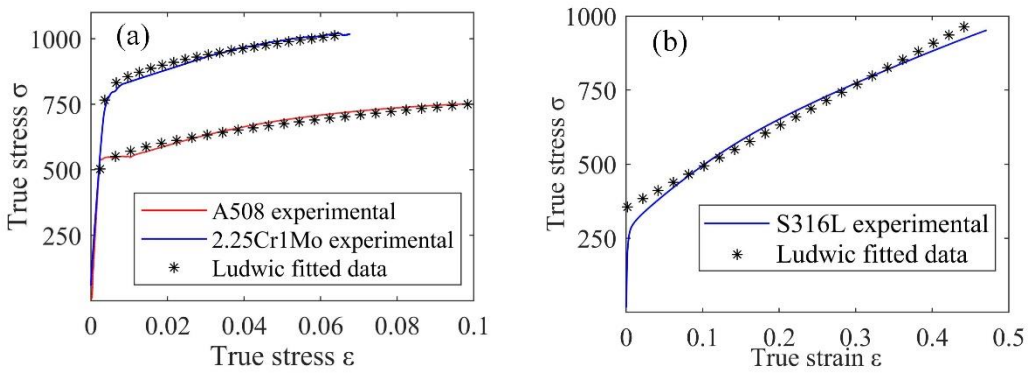

Fig. 5 True stress strain curves extracted from uniaxial tensile tests: (a) A508 and 2.25Cr1Mo; (b) S316L

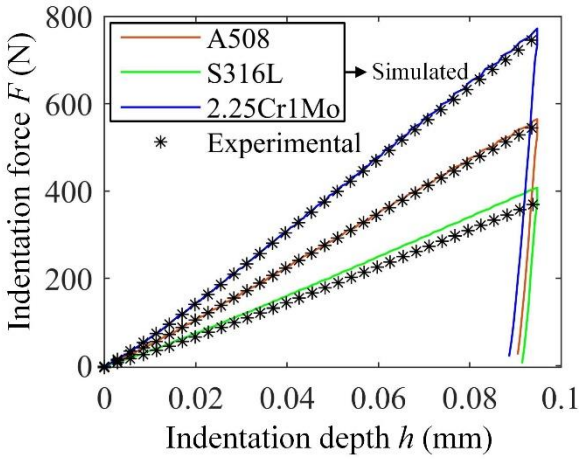

Fig. 6 Indentation force-depth curves measured from experiments and extracted from FE model with material parameters presented.

Table 2 Ludwic parameters of three materials fitted by experimental results

Ludwic parameters	σ_0 (MPa)	K (MPa)	n
A508	503.6	838	0.521
2.25Cr1Mo	766.3	848.1	0.440
S316L	355.8	1381	1

4.2 Prediction of uniaxial flow properties

With the proposed database method, uniaxial flow properties are determined from a single indention F-h curve. Here both indentation force-depth curves extracted from FE model and measured from experiments are employed as the inputs. Actually, many previous studies applied numerical results to validate the accuracy of a new proposed model. The numerical results do not contain noise in experiments and thus can better evaluate the feasibility of the model.

Fig. 7 shows the predicted stresses obtained from the relationship of $f(\boldsymbol{x})$ versus $\sigma_{\varepsilon_i}(\boldsymbol{x})$ when the simulated indentation data of three materials are used as inputs. The solid lines represent fitted results of experimental data. Note that only true stresses before the onset of

necking are extracted. For A508 and 2.25Cr1Mo, the plastic strain are less than 0.1 (seen from Fig. 5 (a)) and for 316L, the value is less than 0.5 (Fig. 5 (b)). To avoid repentance, partial $f(\boldsymbol{x})$ - $\sigma_{\varepsilon_i}(\boldsymbol{x})$ relationships are presented in the figures. It can be seen that the minimum deviation $f(\boldsymbol{x})$ reaches to a level that less than 0.2%, which indicate the $f(\boldsymbol{x})$ - $\sigma_{\varepsilon_i}(\boldsymbol{x})$ relationships show good convergence. Comparisons results show that the predicted stresses of the three materials are in excellent agreement with the fitted tensile data for A508 and 316L. However, the result of S316L (Fig. 7 (c)), indicates the predicted stresses at ε_i=0.2 and 0.4 have bigger errors than others. A possible explanation is that the plastic deformation of region underneath the indenter is constraint by surrounding materials, and thus the overall plastic strain is limited at a small range. Fig. 8 depicts the distribution of equivalent plastic strain of a representative indentation simulation. It is seen that the strain larger than 0.5 is distributed on the region underneath the indenter between 0-45 degrees, taking a small region of the overall volume. Therefore, the flow curves at larger strain has little influence on the indentation F-h curves. When indention curves are used to derive the uniaxial flow properties inversely, larger errors may occur at larger plastic strains.

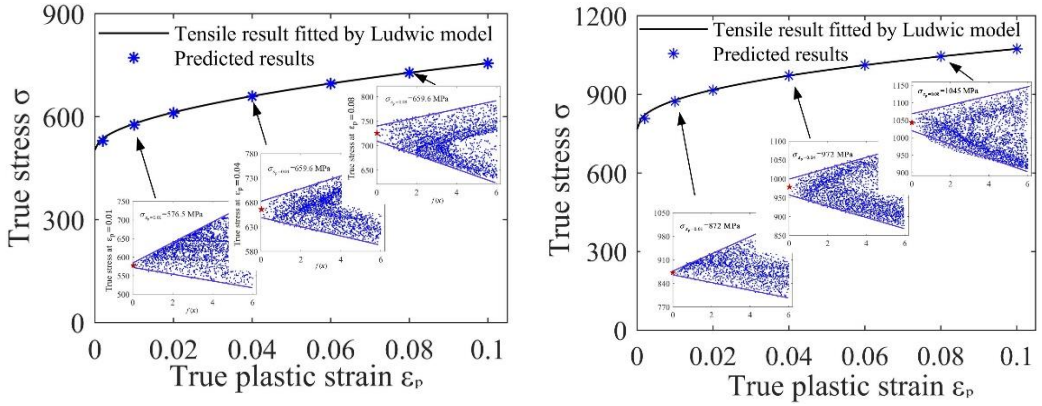

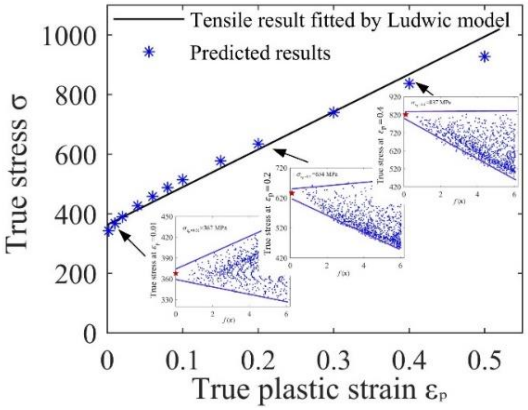

Fig. 7 Flow curves fitted from experimental tensile results and predicted using database method with simulated indentation data as inputs for (a) A508, (b) 2.25Cr1Mo and (c) 316L

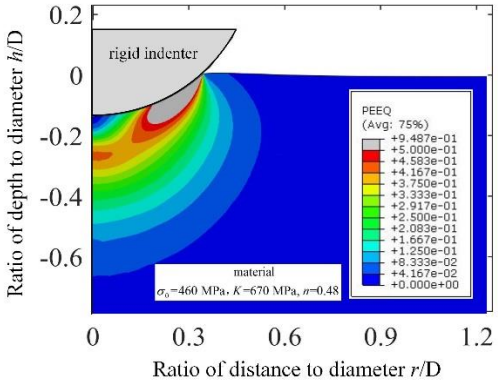

Fig. 8 The distribution of equivalent plastic strain.

Fig. 9 shows the predicted stresses when the experimental indentation *F*-*h* curves of the three materials are used as inputs. The solid lines represent the experimental flow curves. As expected, the minimum $f(\boldsymbol{x})$ is larger than that for simulated curves as inputs, demonstrating that the convergence is inferior to the result of simulated curves as inputs. As explained in previous study [25], when employing the experimental indentation *F*-*h* curves, the quality of the data may be impaired owing to inevitable noise, which results in the intrinsic deviation between the experimental curves and the curves in the database. Nevertheless, Fig. 9 shows that the predicted stress values still follow the experimental flow curves reasonably well.

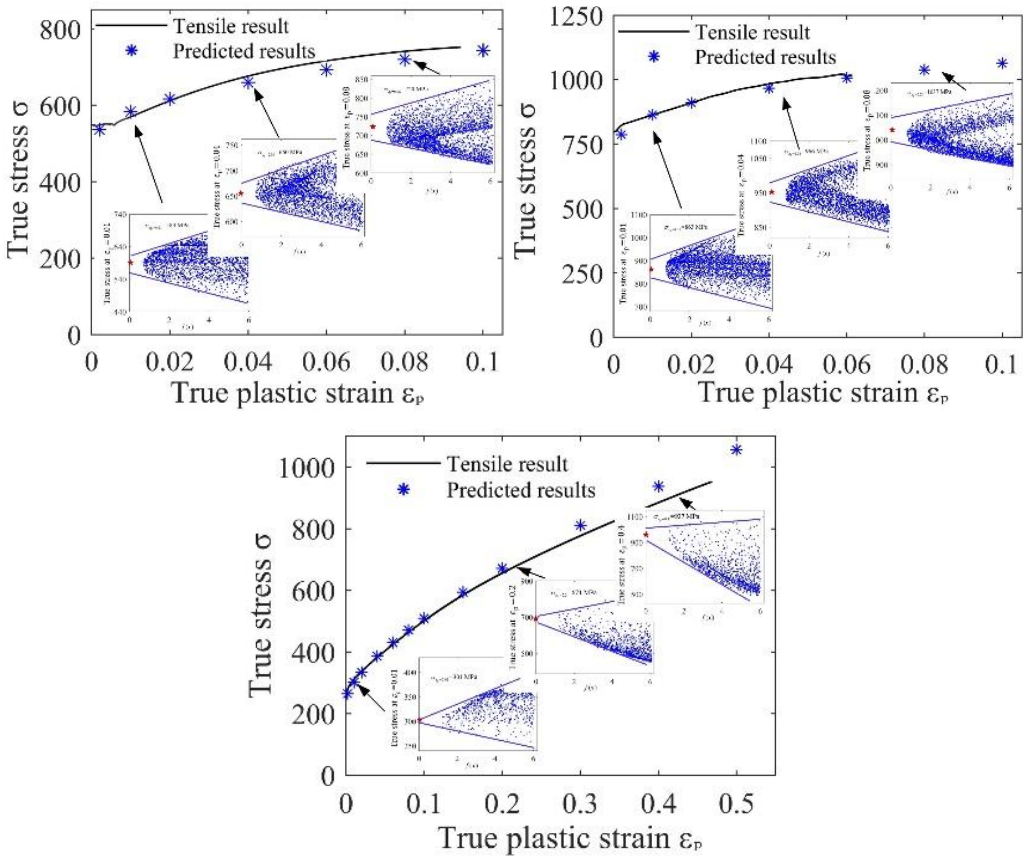

Fig. 9 Flow curves measured from experimental tensile results and predicted using database method with experimental indentation data as inputs for (a) A508, (b) 2.25Cr1Mo and (c) 316L

The material parameters are given in Table 3. As expected, the simulated indentation data provide a more accurate material parameters when compared with the experimental indentation data. Moreover, it is interesting to notice that material parameters from the simulated indentation data have considerable difference with that from the experimental indentation data although the simulated and experimental curves are quite consistent (see Fig. 6). This reveals that when a single indentation *F*-*h* curve are employed to inversely determine the tensile curve, a small difference in *F*-*h* curves may account for a large deviation of the tensile curves. For this reason, high-resolution experimental indentation curves that reflect the true elastic-plastic response of materials is necessary when inverse approaches are used.

From the above discussion, the advantage of this new method is that a database replaced the iterative FE calculations in conventional inverse methods and thus can process the indentation data more quickly and easily. However, it should also be emphasized that the predicted stresses are estimated artificially, which may cause subjective errors.

Table 3. Material parameters fitted from the stress-strain data

	Predicted (input: FE data)			Predicted (input: experimental data)			experimental		
Material	σ_0	K	n	σ_0	K	n	σ_0	K	n
A508	493	834	0.50	495	706	0.46	503	838	0.52
2.25Cr1Mo	736	839	0.39	674	804	0.31	766	848	0.44
316L	379	1155	1	322	1555	1	355	1381	1

5 Conclusion

In the present study, a new approach was suggested for extraction of material uniaxial flow curves by employing a single spherical indentation test incorporated with the database. Three different steels i.e. A508, 2.25Cr1Mo, S316L are employed to validate the accuracy of the proposed approach. To make a comparison research, both experimental and simulated indentation force-depth curves are used as inputs. The following conclusion can be drawn according to the researches above:

1) The database method can provide high-quality predictions when simulated indentation F-h curves are used as inputs. When experimental *F-h* curves are employed, the predicted ability is inferior but follow the tensile flow curves reasonable well.

2) The predictive ability of stresses at larger strain are impaired, since the tensile curves

at larger strain has little contributions to the indentation curves.

3) A small difference in *F*-*h* curves may account for a large deviation of the tensile curves, when inverse approaches are used to determine the tensile curve from a single indentation *F*-*h* curve.

Availability of data and materials

All data generated or analyzed during this study are included in this published article

Authors' contributions

GC and XZ was in charge of the whole trial; GC provide formal analysis and wrote this manuscript; JZ and KG gave the methodology of this manuscript. All authors read and approved the final manuscript.

Funding

This project is funded by the China Postdoctoral Science Foundation (2019M661406).

Competing Interests

The authors declare no competing financial interests.

Acknowledgements

Not applicable

Reference

[1] T.S. Byun, J.H. Hong, F.M. Haggag, K. Farrell, E.H. Lee, Measurement of through-the-thickness variations of mechanical properties in SA508 Gr.3 pressure vessel steels using ball indentation test technique, Int J Pres Ves Pip 74(3) (1997) 231-238.

[2] Y. Yang, W.Q. Wang, M.D. Song, The Measurement of Mechanical Properties of Pipe Steels in Service through Continuous Ball Indentation Test, Procedia Engineering 130 (2015) 1742-1754.

[3] A.R.H. Midawi, C.H.M. Simha, A.P. Gerlich, Assessment of yield strength mismatch in X80 pipeline steel welds using instrumented indentation, Int J Pres Ves Pip 168 (2018) 258-268.

[4] G. Sun, F. Xu, G. Li, X. Huang, Q. Li, Determination of mechanical properties of the weld line by combining micro-indentation with inverse modeling, Computational Materials Science 85 (2014) 347-362.

[5] R. Pamnani, V. Karthik, T. Jayakumar, M. Vasudevan, T. Sakthivel, Evaluation of mechanical properties across micro alloyed HSLA steel weld joints using Automated Ball Indentation, Materials Science and Engineering: A 651 (2016) 214-223.

[6] N. Noii, I. Aghayan, Characterization of elastic-plastic coated material properties by indentation techniques using optimisation algorithms and finite element analysis, International Journal of Mechanical Sciences 152 (2019) 465-480.

[7] M. Bocciarelli, G. Bolzon, Indentation and imprint mapping for the identification of interface properties in film-substrate systems, International Journal of Fracture 155(1) (2009) 1-17.

[8] L.M. Farrissey, P.E. McHugh, Determination of elastic and plastic material properties using indentation: Development of method and application to a thin surface coating, Materials Science and Engineering: A 399(1-2) (2005) 254-266.

[9] J.-Y. Kim, K.-W. Lee, J.-S. Lee, D. Kwon, Determination of tensile properties by instrumented indentation technique: Representative stress and strain approach, Surface and Coatings Technology 201(7) (2006) 4278-4283.

[10] S. Wu, T. Xu, M. Song, K. Guan, Mechanical properties characterisation of welded joint of austenitic stainless steel using instrumented indentation technique, Mater High Temp 33(3) (2016) 270-275.

[11] J.-H. Ahn, D. Kwon, Derivation of plastic stress–strain relationship from ball indentations:

Examination of strain definition and pileup effect, Journal of Materials Research 16(11) (2011) 3170-3178.

[12] S.-K. Kang, Y.-C. Kim, K.-H. Kim, J.-Y. Kim, D. Kwon, Extended expanding cavity model for measurement of flow properties using instrumented spherical indentation, International Journal of Plasticity 49 (2013) 1-15.

[13] H. Chen, L.-x. Cai, Theoretical model for predicting uniaxial stress-strain relation by dual conical indentation based on equivalent energy principle, Acta Mater 121 (2016) 181-189.

[14] Y. Cao, Depth-sensing instrumented indentation with dual sharp indenters: stability analysis and corresponding regularization schemes, Acta Mater 52(5) (2004) 1143-1153.

[15] T. Zhang, S. Wang, W. Wang, A constitutive model independent analytical method in determining the tensile properties from incremental spherical indentation tests (ISITs), International Journal of Mechanical Sciences 148 (2018) 9-19.

[16] O. Iracheta, C.J. Bennett, W. Sun, A holistic inverse approach based on a multi-objective function optimisation model to recover elastic-plastic properties of materials from the depth-sensing indentation test, Journal of the Mechanics and Physics of Solids 128 (2019) 1-20.

[17] L.Y. Huang, K.S. Guan, T. Xu, J.M. Zhang, Q.Q. Wang, Investigation of the mechanical properties of steel using instrumented indentation test with simulated annealing particle swarm optimization, Theoretical and Applied Fracture Mechanics 102 (2019) 116-121.

[18] J. Luo, J. Lin, T.A. Dean, A study on the determination of mechanical properties of a power law material by its indentation force–depth curve, Philosophical Magazine 86(19) (2006) 2881-2905.

[19] J. Luo, J. Lin, A study on the determination of plastic properties of metals by instrumented indentation using two sharp indenters, International Journal of Solids and Structures 44(18-19) (2007) 5803-5817.

[20] C.K.S. Moy, M. Bocciarelli, S.P. Ringer, G. Ranzi, Identification of the material properties of Al 2024 alloy by means of inverse analysis and indentation tests, Materials Science and Engineering: A 529 (2011) 119-130.

[21] A. Atrian, G.H. Majzoobi, S.H. Nourbakhsh, S.A. Galehdari, R. Masoudi Nejad, Evaluation of tensile strength of Al7075-SiC nanocomposite compacted by gas gun using spherical indentation test and neural networks, Advanced Powder Technology 27(4) (2016) 1821-1827.

[22] K. Jeong, H. Lee, O.M. Kwon, J. Jung, D. Kwon, H.N. Han, Prediction of uniaxial tensile flow using finite element-based indentation and optimized artificial neural networks, Materials & Design 196 (2020).

[23] L. Lu, M. Dao, P. Kumar, U. Ramamurty, G.E. Karniadakis, S. Suresh, Extraction of mechanical properties of materials through deep learning from instrumented indentation, Proc Natl Acad Sci U S A 117(13) (2020) 7052-7062.

[24] M. Zhao, N. Ogasawara, N. Chiba, X. Chen, A new approach to measure the elastic–plastic properties of bulk materials using spherical indentation, Acta Mater 54(1) (2006) 23-32.

[25] G. Chen, J. Zhong, X. Zhang, K. Guan, Q. Wang, J. Shi, Estimation of tensile strengths of metals using spherical indentation test and database, Int J Pres Ves Pip 189 (2021).

Figures

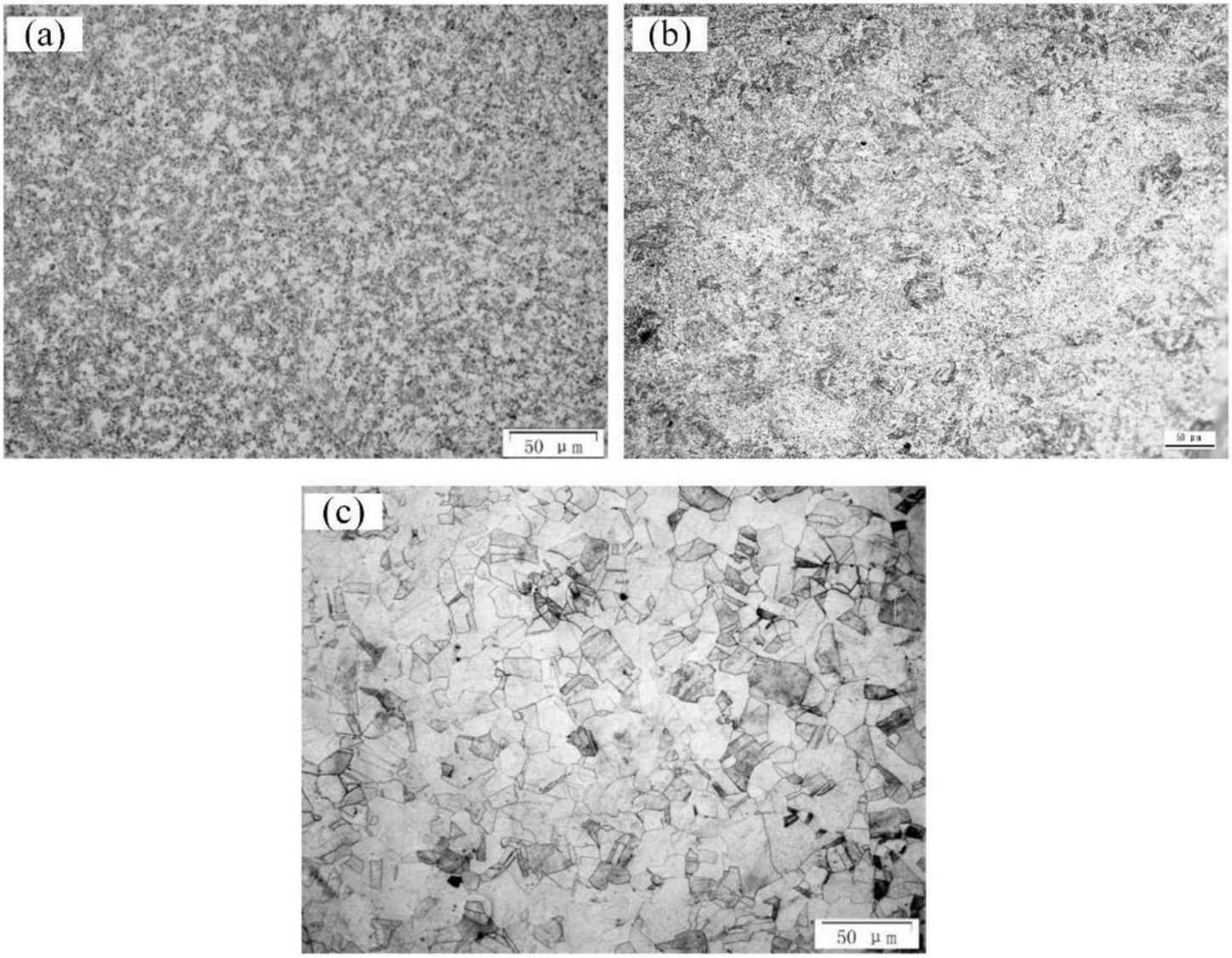

Figure 1

The optical microstructures for (a) A508, (b) 316L and (c) 2.25Cr1Mo

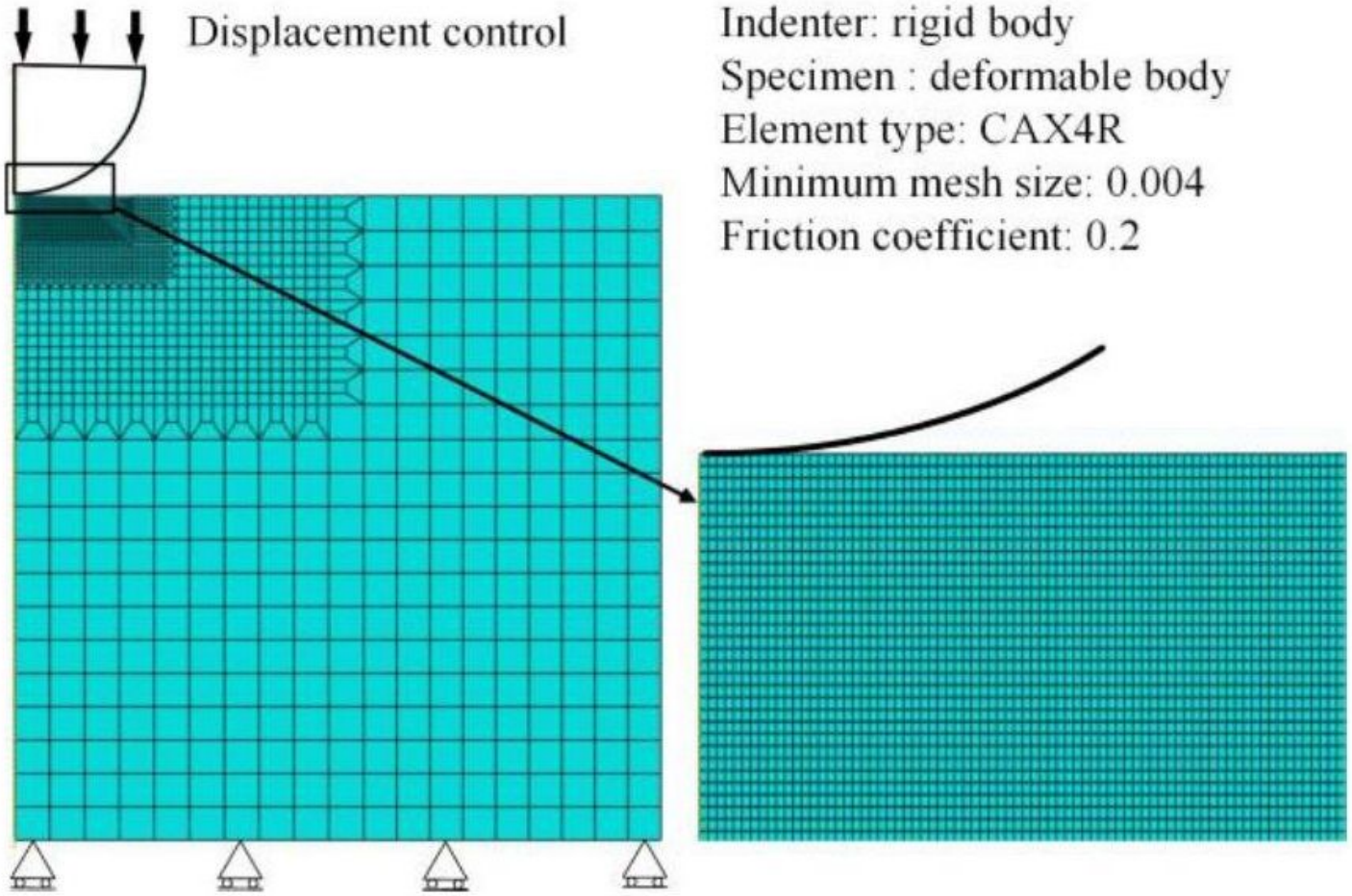

Figure 2

Finite element model of Indentation tests

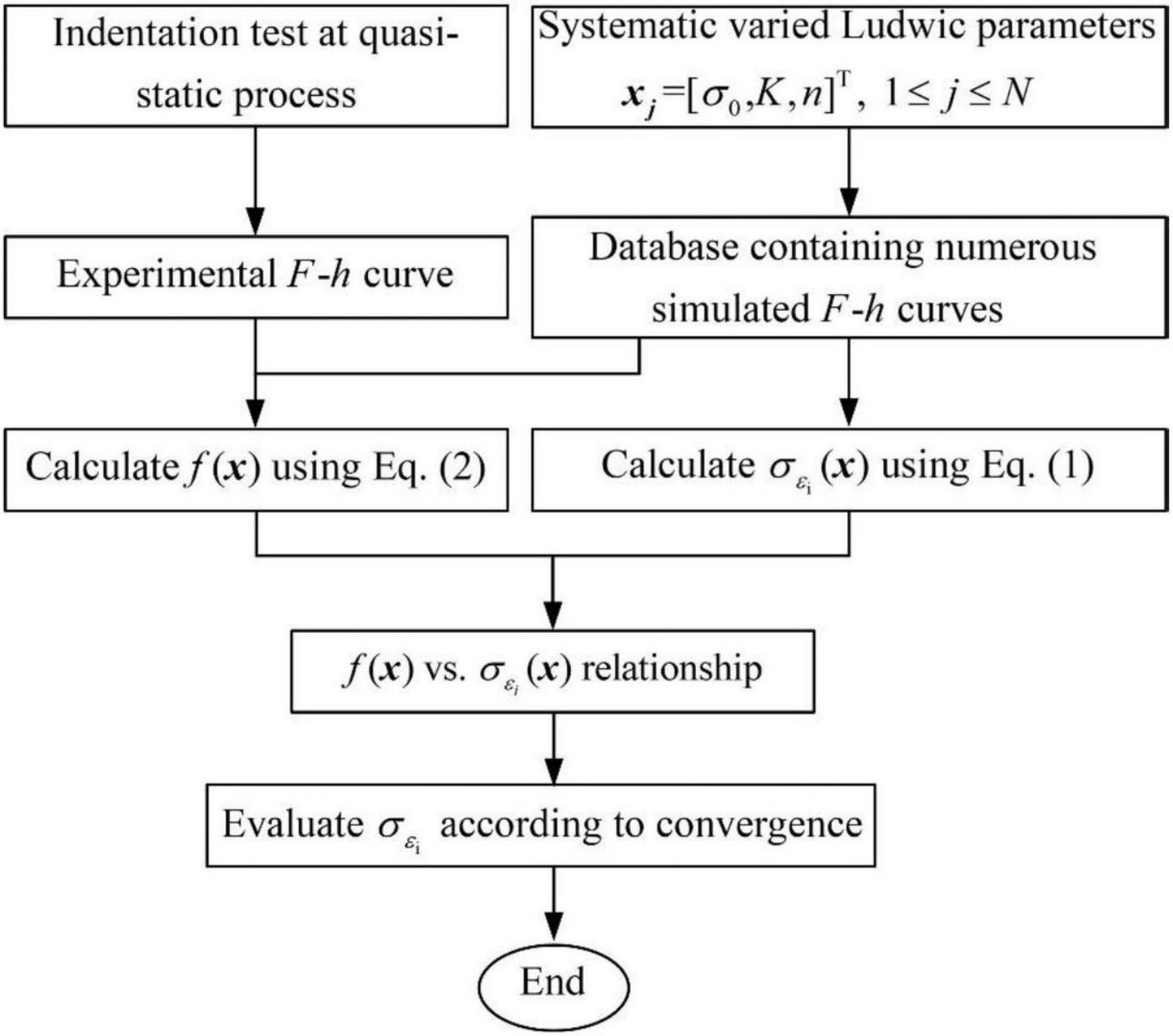

Figure 3

flow chart for the new inverse method to determine the flow properties of metal materials

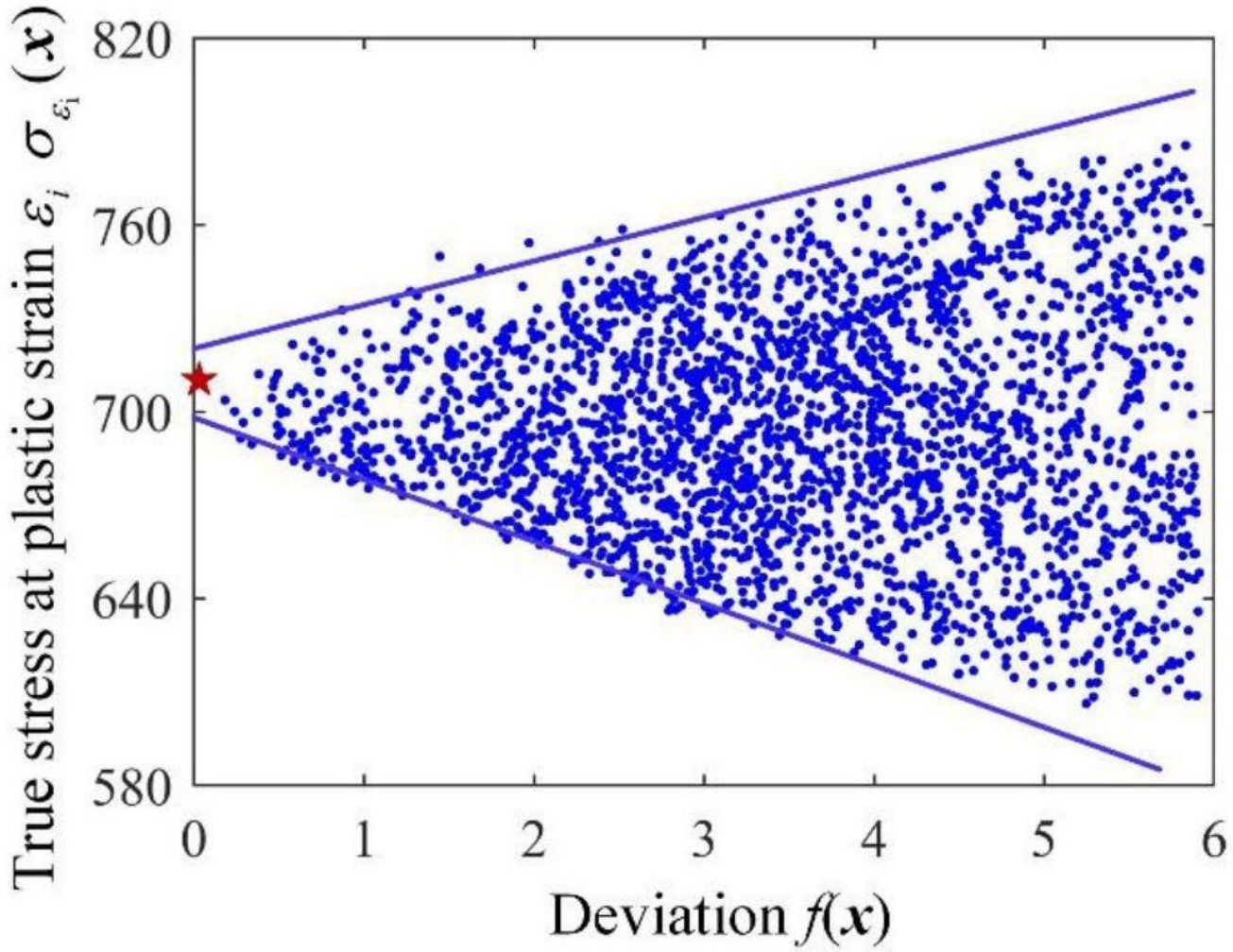

Figure 4

ypical f(x)-σsi(x) relationship indicating convergent σsi(x) with decreasing f(x)

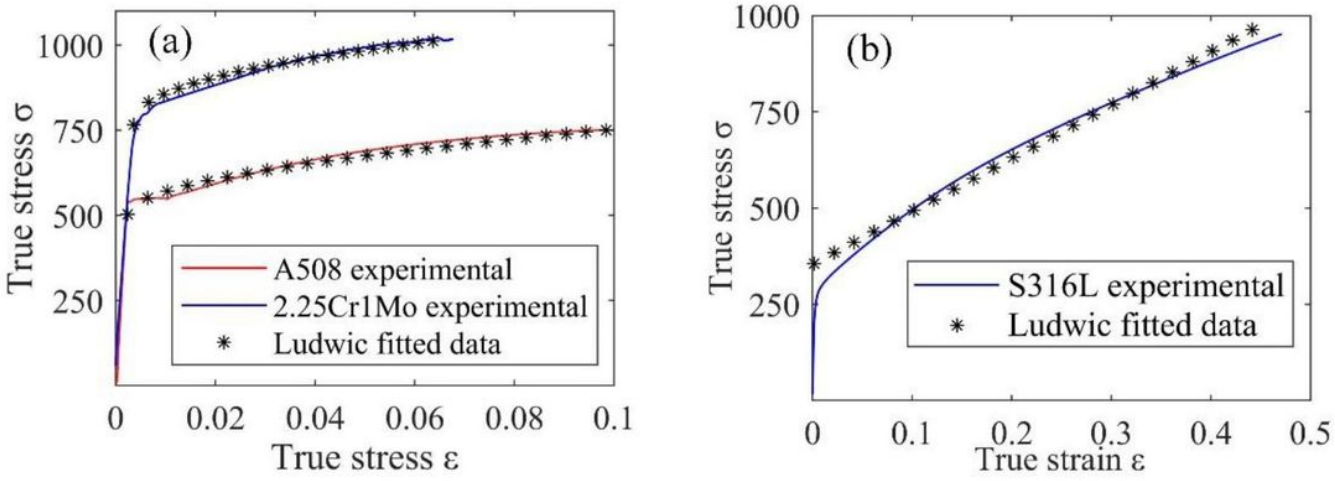

Figure 5

True stress strain curves extracted from uniaxial tensile tests: (a) A508 and 2.25Cr1Mo; (b) S316L

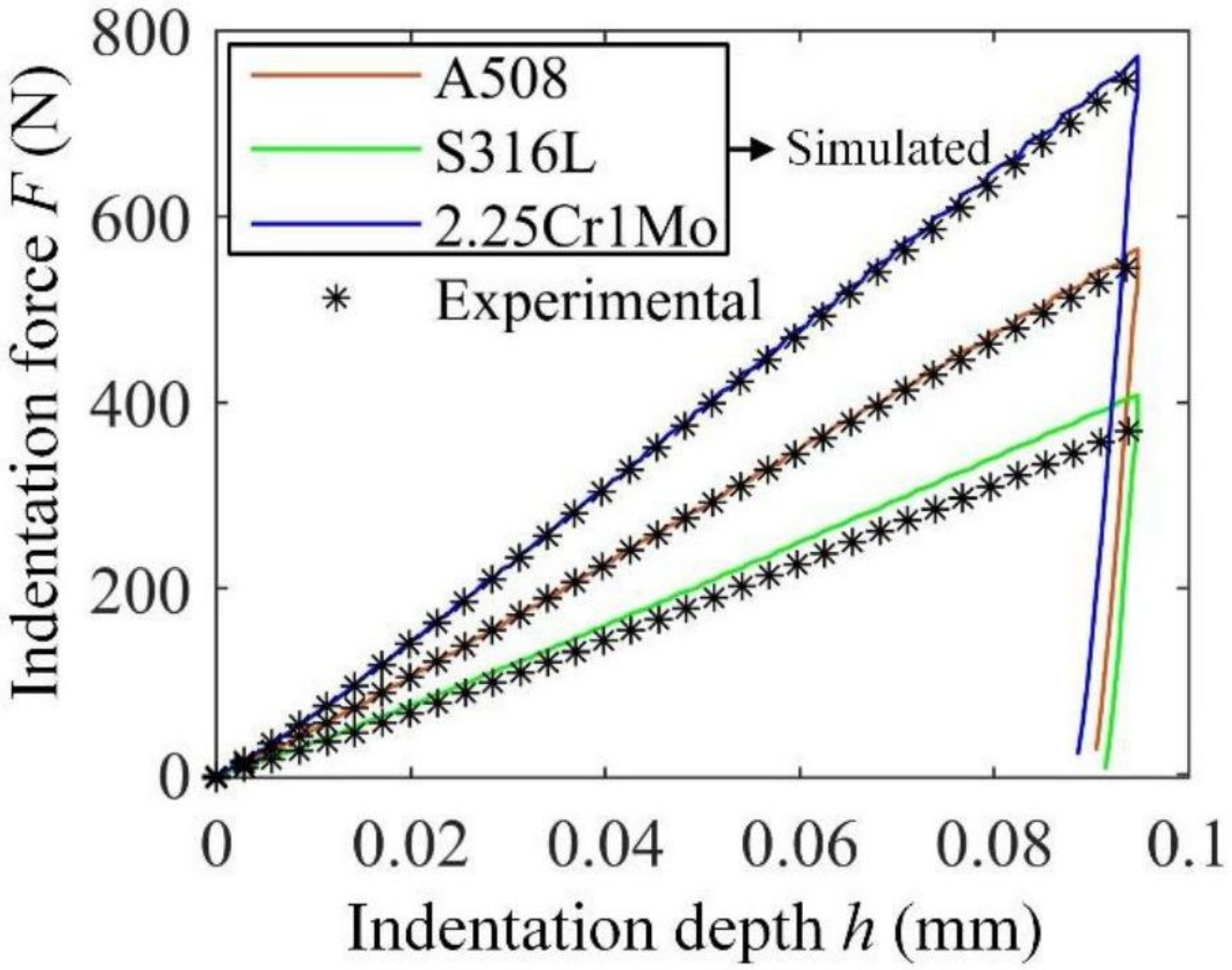

Figure 6

Indentation force-depth curves measured from experiments and extracted from FE model with material parameters presented.

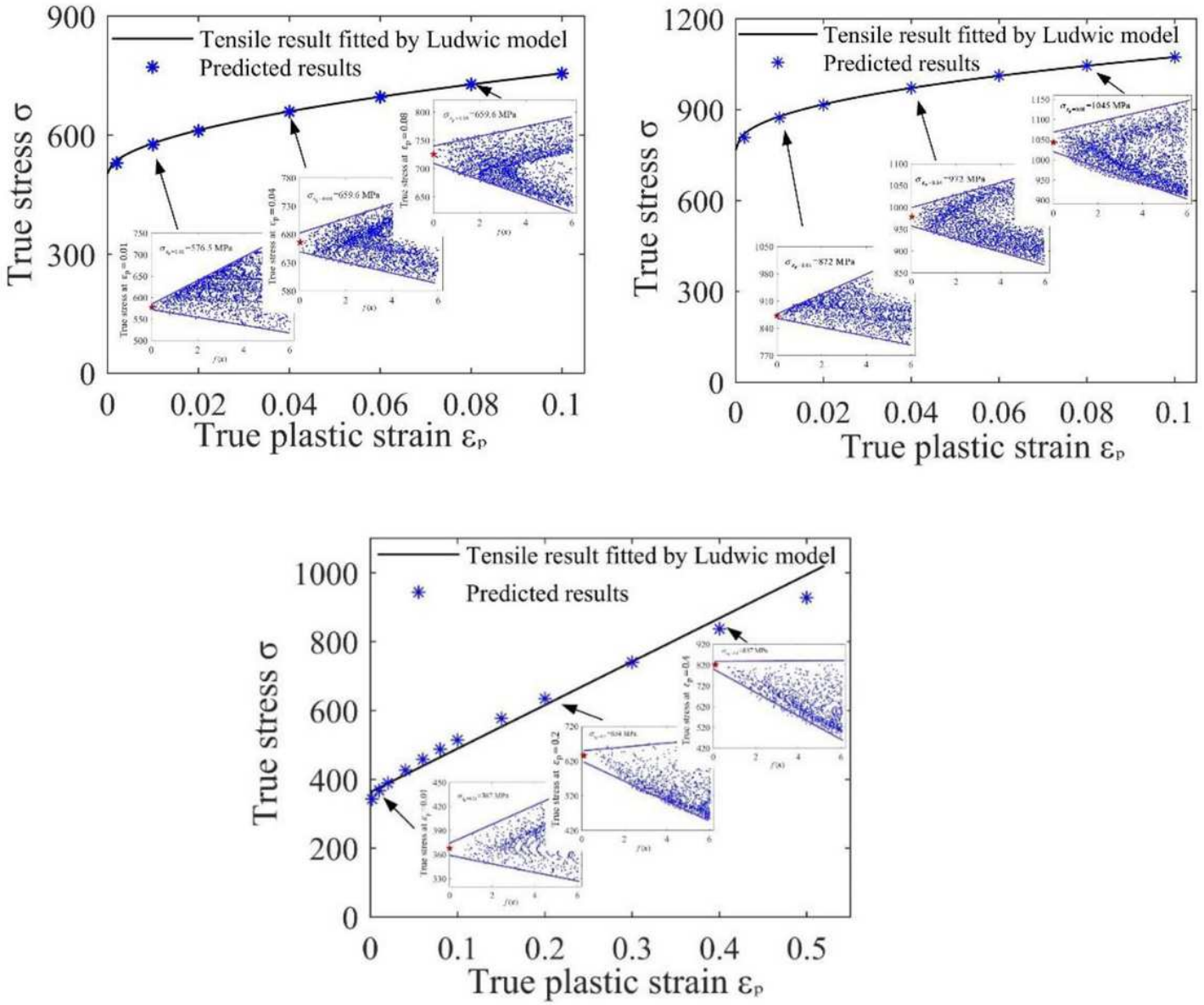

Figure 7

Flow curves fitted from experimental tensile results and predicted using database method with simulated indentation data as inputs for (a) A508, (b) 2.25Cr1Mo and (c) 316L

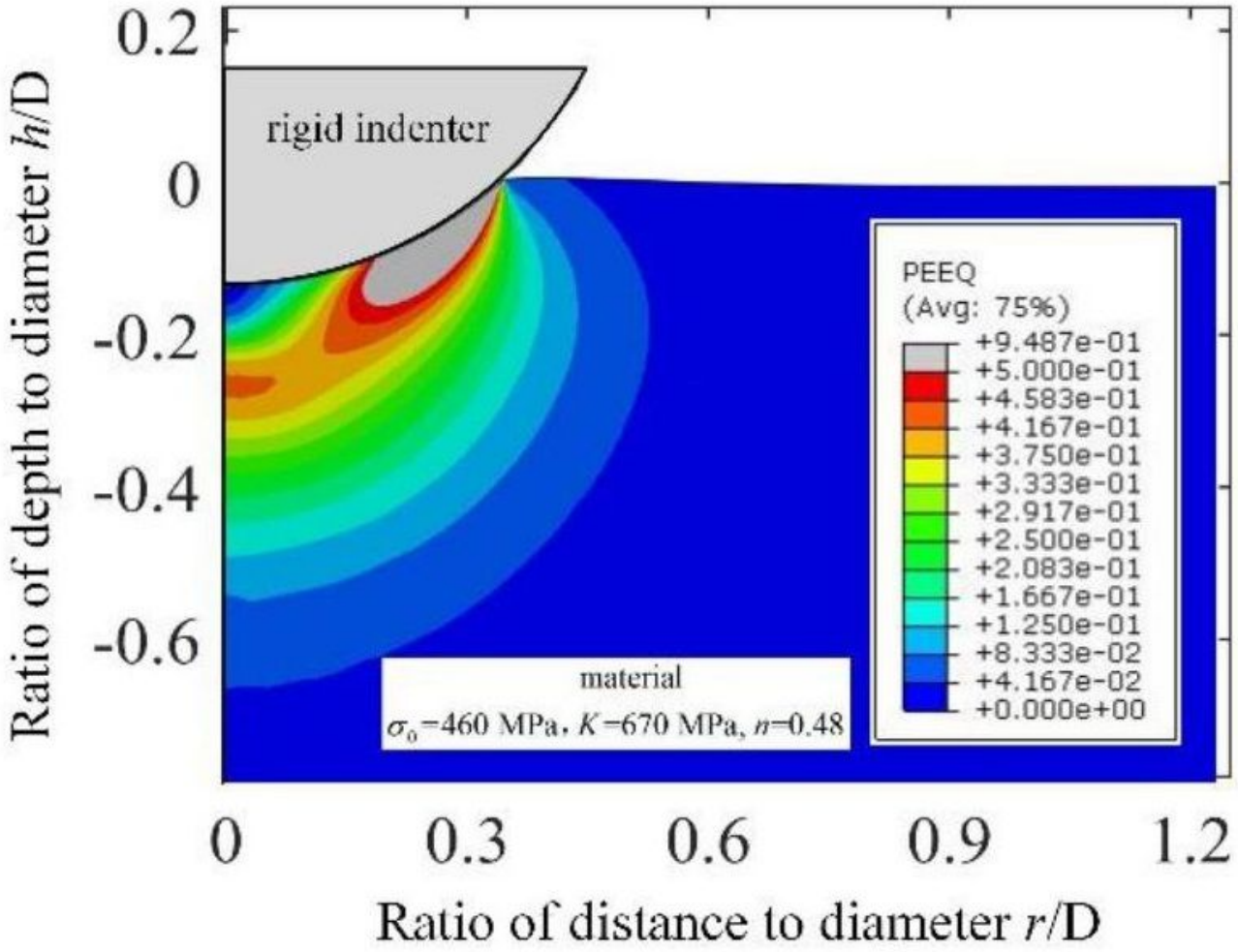

Figure 8

The distribution of equivalent plastic strain.

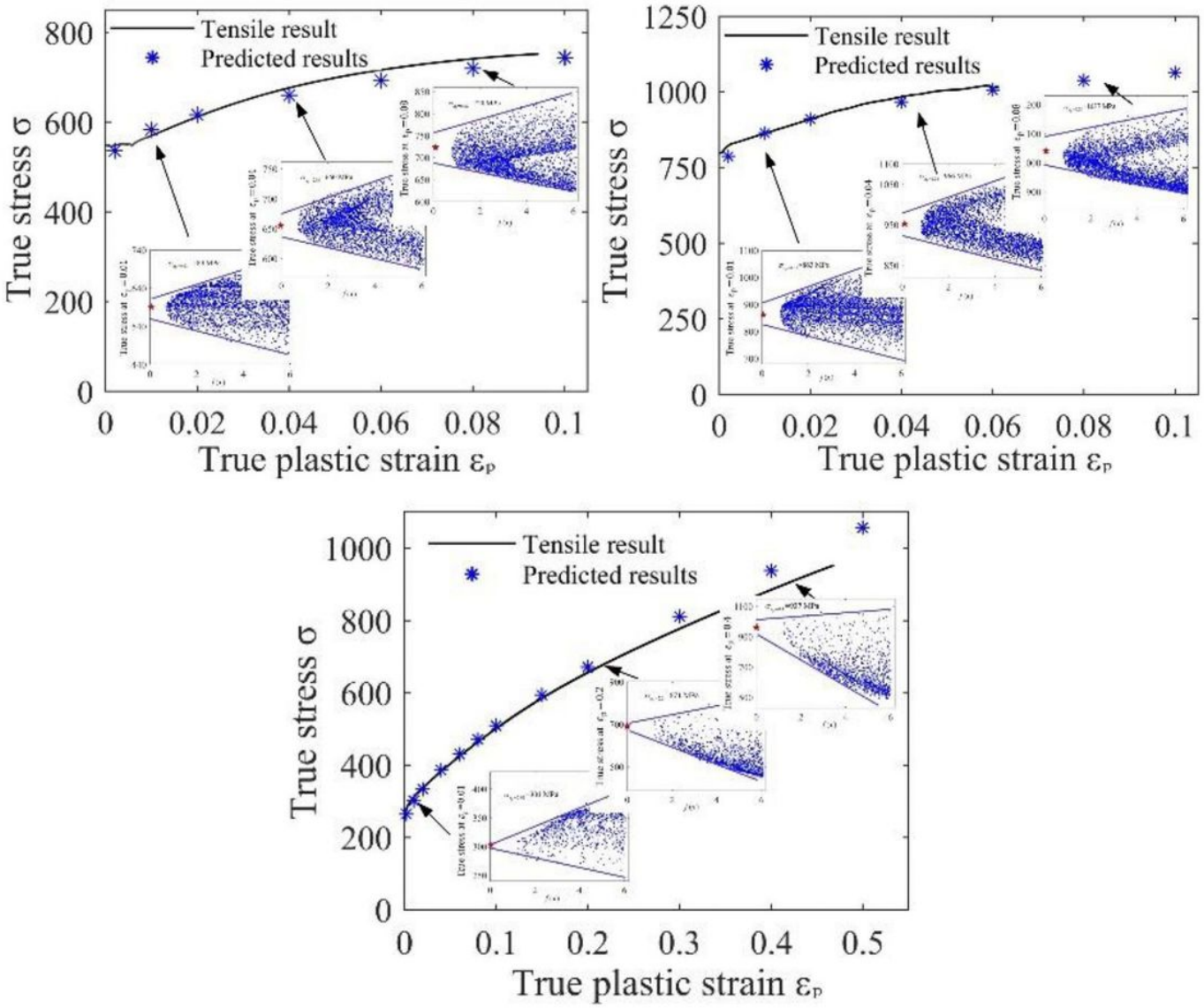

Figure 9

Flow curves measured from experimental tensile results and predicted using database method with experimental indentation data as inputs for (a) A508, (b) 2.25Cr1Mo and (c) 316L